Discovering Matter-Antimatter Asymmetries with GPUs

Stefanie Reichert[1] *on behalf of the LHCb collaboration*

[1]School of Physics and Astronomy, The University of Manchester, Oxford Road, Manchester, M13 9PL, United Kingdom

DOI: http://dx.doi.org/10.3204/DESY-PROC-2014-05/25

The search for matter-antimatter asymmetries requires highest precision analyses and thus very large datasets and intensive computing. This contribution discusses two complementary approaches where GPU systems have been successfully exploited in this area. Both approaches make use of the CUDA THRUST library which can be used on supported GPUs. The first approach is a generic search for local asymmetries in phase-space distributions of matter and antimatter particle decays. This powerful analysis method has never been used to date due to its high demand in CPU time. The second approach uses the GOOFIT framework, which is a generic fitting framework that exploits massive parallelisation on GPUs.

1 Introduction

In the neutral charm meson system, the mass eigenstates or physical particles $|D_{1,2}\rangle$ with masses $m_{1,2}$ and widths $\Gamma_{1,2}$ are a linear combination of the flavour eigenstates $|D^0\rangle$ and $|\bar{D}^0\rangle$ which govern the interaction. The linear combination $|D_{1,2}\rangle = p|D^0\rangle \pm q|\bar{D}^0\rangle$ depends on complex coefficients q, p satisfying the normalisation condition $|q|^2+|p|^2 = 1$. The flavour eigenstates are subject to matter-antimatter transitions, so-called mixing, through box diagrams as illustrated in Fig. 1.

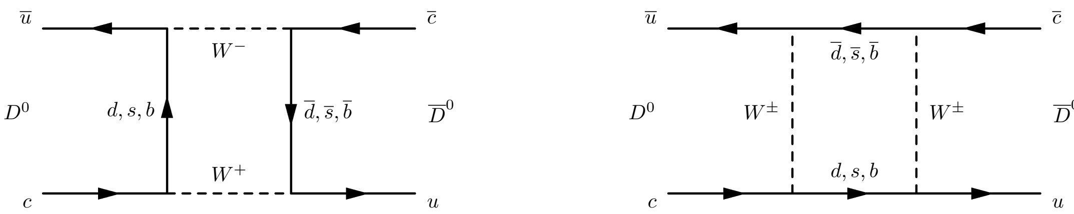

Figure 1: (Left) Box diagram for $D^0 - \bar{D}^0$ mixing via intermediate $W^\pm$ bosons and (right) via intermediate quarks.

The $D^0 - \bar{D}^0$ oscillation is driven by a non-zero difference in masses and widths of the mass eigenstates $\Delta m = m_2 - m_1$ and $\Delta\Gamma = \Gamma_2 - \Gamma_1$, respectively. The mixing parameters x and y are defined as $x = \Delta m/\Gamma$ and $y = \Delta\Gamma/(2\Gamma)$ where Γ denotes the width average $\Gamma = (\Gamma_1 + \Gamma_2)/2$ of the mass eigenstates. The mass eigenstates are eigenstates to the charge-parity (CP) operator if $CP|D_{1,2}\rangle = \pm|D_{1.2}\rangle$ is fulfilled. Three different types of CP violation can be distinguished. CP violation in decay is implied if the decay amplitude of a D^0 to a final state f and the amplitude of the charge conjugated $\bar{D}^0 \to \bar{f}$ decay differ. In case of $|q/p| \neq 1$, the CP operator transforms the mass eigenstates to states which are not CP eigenstates. This phenomenon is know as CP violation in mixing. Furthermore, CP violation in decay and mixing can interfere. In the charm sector, mixing is well established, while no evidence of CP violation has been measured [1].

The mixing parameters in the charm sector are of the order $\mathcal{O}(10^{-3})$ due to the small mass and width differences Δm and $\Delta\Gamma$ of the mass eigenstates. Therefore, measurements of the charm mixing parameters and searches for CP violation are experimentally challenging and are required to be performed on large datasets. The datasets recorded at the LHCb experiment [2] used for such measurements contain typically several millions of events. Most analysis methods are CPU-expensive but are parallelisable and benefit from the massive parallelisation and speed-up provided by the usage of GPUs. In particular, the presented methods rely on the CUDA THRUST library [3] providing similar functionalities as the C++ Standard Template Library (STL). Functions available in STL such as reduce are also part of the CUDA THRUST library which also enables portability between GPUs and multicore CPUs.

2 Energy test for $D^0 \to \pi^+\pi^-\pi^0$ using the CUDA Thrust library

The energy test [4] is an unbinned model-independent statistical method to search for time-integrated CP violation in $D^0 \to \pi^+\pi^-\pi^0$ decays (charge conjugate decays are implied unless stated otherwise). The method relies on the comparison of two D^0 and $\bar{D}^0$ flavour samples and is sensitive to local CP asymmetries across phase-space. The phase-space is spanned by the invariant mass squared of the daughter particles, e.g. by $m^2(\pi^+\pi^0)$ and $m^2(\pi^-\pi^0)$. The $D^0 \to \pi^+\pi^-\pi^0$ decay is required to originate from a $D^{*+} \to D^0\pi^+$ decay. By determining the charge of the soft pion of the $D^{*+} \to D^0\pi^+$ decay, the data are split in two independent samples containing either D^0 or $\bar{D}^0$ candidates. For both samples, a test statistic T is computed as

$$T \approx \sum_{i}^{n}\sum_{j>i}^{n}\frac{\psi\left(\Delta\vec{x}_{ij}\right)}{n^2-n} + \sum_{i}^{\bar{n}}\sum_{j>i}^{\bar{n}}\frac{\psi\left(\Delta\vec{x}_{ij}\right)}{\bar{n}^2-\bar{n}} - \sum_{i}^{n}\sum_{j}^{\bar{n}}\frac{\psi\left(\Delta\vec{x}_{ij}\right)}{n\bar{n}}, \tag{1}$$

where $n(\bar{n})$ is the size of the $D^0(\bar{D}^0)$ sample, $\psi\left(\Delta\vec{x}_{ij}\right)$ is a metric function and $\Delta\vec{x}_{ij}$ is the distance in the 3-dimensional phase-space between events i and j. A Gaussian, given by

$$\psi\left(\Delta\vec{x}_{ij}\right) = e^{-\Delta\vec{x}_{ij}^2/2\sigma^2}, \tag{2}$$

is chosen as metric function. The width σ is tunable and indicates the radius in which the method is sensitive to local phase-space asymmetries. Thus, σ should be larger than the resolution of $\Delta\vec{x}_{ij}$ and small enough to avoid a dilution of locally varying asymmetries. The three terms in Eq. 1 are the average distance in the D^0, $\bar{D}^0$ and mixed sample. In case of large CP asymmetries, the T-value increases. The T-value computation uses *thrust::transform_reduce* from the CUDA THRUST library to compute the sums in 1. The function *thrust::transform_reduce* performs a reduction operation, e.g. an addition, after an application of an operator to each element of an input sequence. In this analysis, for each point, the Gaussian metric function having been initialised with the position of event i is evaluated with respect to the position of event j.

The measured T-value does not indicate the presence of CP violation on its own and needs to be compared with the hypothesis of no CP violation. So-called permutation samples are generated where the flavour of each D^0 and $\bar{D}^0$ candidate is reassigned randomly. The permutation samples then reflect the no CP violation hypothesis. The T-value of each permutation sample is calculated resulting in a distribution of T-values reflecting the no CP violation hypothesis. A p-value for the no CP violation hypothesis is calculated as the fraction of permutation T-values greater than the measured T-value. In case that the measured T-value lies outside the range of the permutation T-value distribution, the latter is fitted with a generalised extreme value function [5, 6]

$$f(x;\mu,\sigma,\xi) = N\left[1+\xi\left(\frac{x-\mu}{\sigma}\right)\right]^{(-1/\xi)-1}\exp\left\{-\left[1+\xi\left(\frac{x-\mu}{\sigma}\right)\right]^{-1/\xi}\right\}, \tag{3}$$

where N is the normalisation, μ the location, σ the scale and ξ the shape parameter. The p-value is then defined as the fraction of the integral above the measured T-value. A statistical uncertainty on the p-value is obtained by propagating the uncertainties on the fit parameters or in case of counting as a binomial standard deviation. On a sample of 700,000 candidates, which is of the same order as the analysed data set of $663,000$ selected events, the energy test with a single permutation requires approximately 10 hours of CPU time whereas the GPU implementation of the energy test runs in 11 minutes. To obtain a reliable p-value, around 1000 permutation samples reflecting the no CP violation hypothesis are required. The results of the energy test on a data sample of $\mathcal{L}_{\text{int}} = 2\,\text{fb}^{-1}$ recorded at a centre-of-mass energy of 8 TeV are summarised in Table 1 for various metric parameter values. Monte-Carlo studies indicate that $\sigma = 0.3\,\text{GeV}^2$ yields the best sensitivity. The permutation T-value distribution and the measured T-value are illustrated in Fig. 2 along with the visualisation of the asymmetry significance which is obtained by assigning an asymmetry significance to each event similar to the T-value extraction. The analysed data set are found to be consistent with a no CP violation hypothesis at a probability of $(2.6 \pm 0.5)\%$ [7].

σ [GeV^2]	p-value
0.2	$(4.6 \pm 0.6) \times 10^{-2}$
0.3	$(2.6 \pm 0.5) \times 10^{-2}$
0.4	$(1.7 \pm 0.4) \times 10^{-2}$
0.5	$(2.1 \pm 0.5) \times 10^{-2}$

Table 1: p-values for various metric parameter values. The p-values are obtained with the counting method [7].

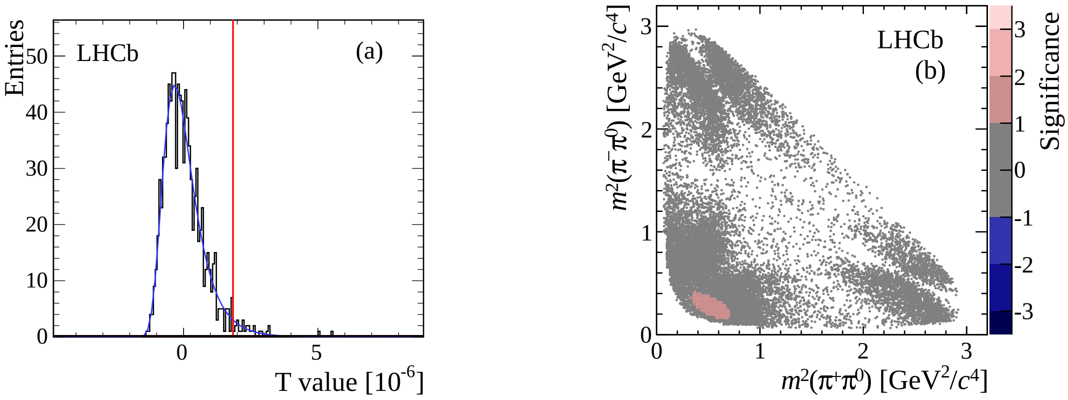

Figure 2: (Left) Permutation T-value distribution and the resulting the fit function. The measured T-value is indicated by the vertical line. (Right) Visualisation of local asymmetry significances. The negative (positive) asymmetry significance is set for the D^0 candidates having negative (positive) contribution to the measured T-value, respectively. The results are given for $\sigma = 0.3\,\text{GeV}^2$ [7].

3 Time-dependent amplitude analysis of $D^0 \to K^0_S\pi^+\pi^-$ with GooFit

A time-dependent amplitude analysis of $D^0 \to K^0_S\pi^+\pi^-$ decays grants direct access to the mixing parameters x and y and allows to search for CP violation in mixing. The three-body decay $D^0 \to K^0_S\pi^+\pi^-$ is treated as a two-body decay $D^0 \to Rc$ through an intermediate resonance $R \to ab$ with the amplitude

$$\begin{aligned}\mathcal{M}_R = \quad & Z(J, L, l, \vec{p}, \vec{q}) B_L^{R\to ab}(|\vec{q}|) \cdot \\ & \mathcal{T}_R(m_{ab}) B_L^{D\to Rc}(|\vec{p}|),\end{aligned} \tag{4}$$

where the angular distribution of the final state particles is denoted by $Z(J = 0, L, l, \vec{p}, \vec{q})$ [8]. For a D^0 meson, $J = 0$, L and l are referring to the orbital angular momentum between R and c and between a and b, respectively. The momenta of c and a in the rest frame of the intermediate resonance R are denoted by $\vec{p}$ and $\vec{q}$. The Blatt-Weißkopf barrier factors [9, 10] are denoted by $B_L(q)$. The dynamical function $\mathcal{T}_R$ is the propagator for the chosen line shape of the resonance, e.g. the Gounaris-Sakurai propagator [11]. A model-dependence of the analysis arises from the choice of intermediate resonances and their line shapes. The two most common models are the so-called isobar model where the line shapes of the resonances in Table 2. are relativistic Breit-Wigners with exception of the $\rho(770)$ which is modelled by a Gounaris-Sakurai shape. An alternative model where the $K^0_S\pi^\pm$ S-waves are described by the LASS parameterisation [12] and the $\pi^+\pi^-$ S-wave is formulated with the K-matrix algorithm LASS parameterisation and K-matrix algorithm preserve unitarity by construction in opposition to the unitarity-violating Breit-Wigner line shapes.

The analysis uses the GooFit [14] library to perform the time-dependent Dalitz-plot (Tddp) amplitude analysis fit. The GooFit package is a parallel fitting framework implemented in CUDA and using the Thrust library. GooFit can be run under OpenMP or on GPUs supporting CUDA. In this framework, the most commonly used line shapes for resonance are available, e.g. Breit-Wigner, Gounaris-Sakurai and the LASS parameterisation as well as the Blatt-Weißkopf barrier factors and angular functions. The K-matrix algorithm to describe the $\pi^+\pi^-$ S-wave is under development. In GooFit, the class *TddpPdf* is dedicated to time-dependent amplitude analyses. The user defines the resonances and line shapes entering the probability density function which is then build in *TddpPdf* and is used as fit model to extract the mixing parameters x and y. The *TddpPdf* class requires the invariant mass squared of two daughter pair combinations, the D^0 decay time and its uncertainty as well as the event number as input. In addition to the amplitude model, background components, efficiencies and resolutions can be included in the fit. The framework allows to veto certain regions in phase-space and the blinding of results. The Thrust library is used to compute the amplitudes of the intermediate resonances and the matrix elements contributing to the logarithm of the likelihood. In addition, the computation of the normalisation integral of the fit model relies heavily on *thrust::transform*, *thrust::transform_reduce*, *thrust::make_zip_iterator* and *thrust::make_tuple*. For example, *thrust::transform_reduce* is used to loop over an input sequence created by *thrust::make_zip_iterator* which yields a sequence of tuples from multiple tuples returned by *thrust::make_tuple*. For each element of this sequence, the phase-space integral is computed which is then added to a complex number to yield the total phase-space integral. Due to the parallelisation with the methods from the Thrust library, the fit runs over several hundred thousand or million of events in minutes instead of hours. In Fig. 3, the results of an amplitude analysis fit of a toy data sample generated according to the isobar model with $x = y = 0.005$ is shown.

Resonance R	Mass [GeV]	Width [GeV]	Spin
$R \to \pi^+\pi^-$			
$\rho(770)$	0.776	0.146	1
ω	0.783	0.008	1
$f_0(980)$	0.975	0.044	0
$f_0(1370)$	1.434	0.173	0
$f_2(1270)$	1.275	0.185	2
σ_1	0.528	0.512	1
σ_2	1.033	0.099	0
$R \to K^0_S\pi^+$			
$K^*(892)^+$	0.894	0.046	1
$K^*_0(1430)^+$	1.459	0.175	0
$K^*_2(1430)^+$	1.426	0.099	2
$R \to K^0_S\pi^-$			
$K^*(892)^-$	0.894	0.046	1
$K^*_0(1430)^-$	1.459	0.175	0
$K^*_2(1430)^-$	1.426	0.099	2
$K^*(1680)^-$	1.677	0.205	1
non-resonant $K^0_S\pi^+\pi^-$			

Table 2: Intermediate resonances contributing to the isobar model with their mass, width and spin. The numbers and the model are taken from the D0mixDalitz model as implemented in EvtGen [13].

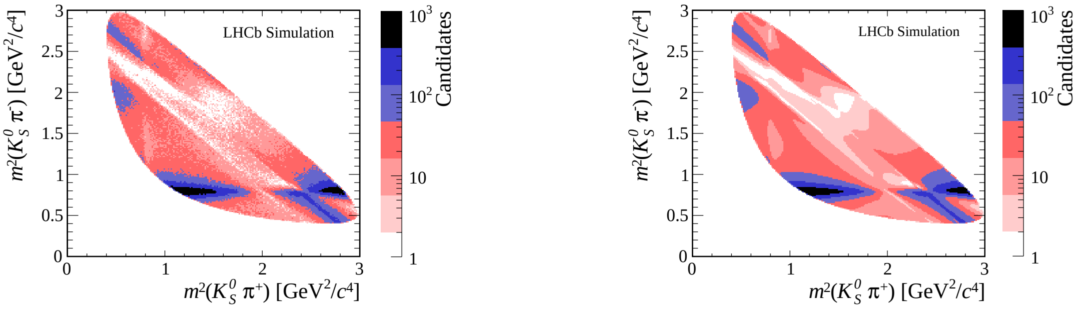

Figure 3: (Left) Toy data and (right) fit model of a toy data sample reflecting the 2012 data taking conditions of LHCb including an efficiency parametrisation. The sample is generated according to the isobar model with $x = y = 0.005$.

4 Conclusion

Searches for CP violation and measurements of the mixing parameters in the charm sector require large statistics which will keep increasing in the future. The search for time-integrated CP violation in $D^0 \to \pi^+\pi^-\pi^0$ decays at LHCb with the energy test is the first analysis at LHCb exploiting the potential provided by GPUs. The energy test could be applied to data for the first time due to the massive parallelisation and reduction of the computing time. A measurement of the mixing parameters x and y with a time-dependent amplitude analysis of $D^0 \to K_S^0\pi^+\pi^-$ decays is currently ongoing with the GooFit package.

References

[1] Y. Amhis et al. Averages of B-Hadron, C-Hadron, and tau-lepton properties as of early 2012 and online update at `http://www.slac.stanford.edu/xorg/hfag`. *arXiv: 1207.1158 [hep-ex]*, 2012.

[2] A.A. Alves Junior et al. The LHCb Detector at the LHC. *JINST*, 3:S08005, 2008.

[3] The Thrust libraries. `https://thrust.github.io/`.

[4] M. Williams. Observing CP Violation in Many-Body Decays. *Phys.Rev.*, D84:054015, 2011.

[5] B. Aslan and G. Zech. New test for the multivariate two-sample problem based on the concept of minimum energy. *JSCS*, 75(2):109, 2005.

[6] B. Aslan and G. Zech. Statistical energy as a tool for binning-free, multivariate goodness-of-fit tests, two-sample comparison and unfolding. *Nucl. Instr. Meth. Phys. Res. A*, 537(3):626, 2005.

[7] R. Aaij et al. Search for CP violation in $D^0 \to \pi^-\pi^+\pi^0$ decays with the energy test. *arXiv:1410.4170 [hep-ex]*, 2014.

[8] J. Beringer et al. Review of Particle Physics (RPP). *Phys.Rev.*, D86:010001, 2012.

[9] J. Blatt and V. Weisskopf. *Theoretical Nuclear Physics.* John Wiley & Sons, 1952.

[10] F. Von Hippel and C. Quigg. Centrifugal-barrier effects in resonance partial decay widths, shapes, and production amplitudes. *Phys.Rev.*, D5:624, 1972.

[11] G.J. Gounaris and J.J. Sakurai. Finite width corrections to the vector meson dominance prediction for $\rho \to e^+e^-$. *Phys.Rev.Lett.*, 21:244, 1968.

[12] D. Aston et al. A Study of $K^-\pi^+$ Scattering in the Reaction $K^-p \to K^-\pi^+n$ at 11-GeV/c. *Nucl.Phys.*, B296:493, 1988.

[13] D. J. Lange. The EvtGen particle decay simulation package. *Nucl. Instrum. Meth.*, A462:152, 2001.

[14] The GooFit package. `https://github.com/GooFit/GooFit`.